Exploring the Nature of ULX X-3 in NGC4258

Aysun Akyuz[1], Hasan Avdan[1], Şenay Avdan[1], Nazım Aksaker.[2], Solen Balman[3]

[1]Dept. of Physics, University of Cukurova, Adana, Turkey ; [2]Technical Sciences of Vocational School, University of Cukurova, Adana, Turkey ; [3]Dept. of Physics, Middle East Technical University, Ankara, Turkey

ASTRACT

We present the X-ray and optical properties of the Ultraluminous X-ray Source (ULX) X-3 in the nearby galaxy NGC 4258. Observations of ULX X-3 in the archive that have been carried out with Chandra , XMM-Newton, Swift and Hubble Space Telescope (HST) .

We fitted each X-ray spectrum with a simple power law and multicolor disk blackbody models. The source has a peak luminosity of $L_X \sim 5.4 \times 10^{39}$ erg s[-1] in the Chandra observation however, the luminosity of the source changes a factor of ~ 3 throughout the observations. We have seen no evidence for a possible state transition or spectral variation throughout the X-ray observations. Consideration of the luminosity and spectral properties of the source indicates that the mass of the compact object ~ 15 $M_\odot$. The position of the ULX X-3 on the HST/ACS/WFC images was derived as a result of relative astrometric between Chandra and HST. After carefully examining the images of F435W, F555W and F814W filters three possible candidates have been identified within the error radius of 0.2 arcsec. The counterpart candidates have absolute magnitudes in the range M_V = (-4.8) – (-5.8). The possible spectral types of the candidates from brightest to dimmest were determined as A0-A7, F2-F8, and A3-A5.

INTRODUCTION

ULXs are variable, nonnuclear X-ray sources with isotropic luminosities ($L_X > 10^{39}$ erg s[-1]) above the Eddington limit for a 10 $M_\odot$ black hole. Current models propose several alternatives to explain their high luminosities: It could either stellar-mass black holes accreting at super-Eddington rates [1] or intermediate-mass black holes (IMBHs) of 10^2–10^4 $M_\odot$ with standard accretion discs [2],[3]. On the other hand, three ULXs exhibited pulsed X-ray emission as expected from neutron stars (M82 X-2)[4] , NGC5907 ULX-1 [5] and NGC 7793 P13 [6] . The true nature of ULX binary systems is still unknown.

Studying the X-ray spectral states and state transitions of ULXs with the multi-epoch data and comparing them with the well-known characteristics of Galactic BH binaries (BHB) are essential tools for understanding the radiative mechanisms of these sources. There are three active states that have been defined for Galactic BHBs: thermal, hard, and steep power law (PL) [7].

NGC 4258 (M106) is a nearby (7.7 Mpc, [8] Seyfert-type spiral galaxy. It is well known for its anomalous arms, discovered on the basis of Hα imaging [9]. The source X-3 was classified as a ULX by [8] and also was studied its X-ray spectrum and the temporal properties based on the XMM-Newton observations with the longest exposure [10]. Three color SDSS image of the galaxy is shown in Fig 1.
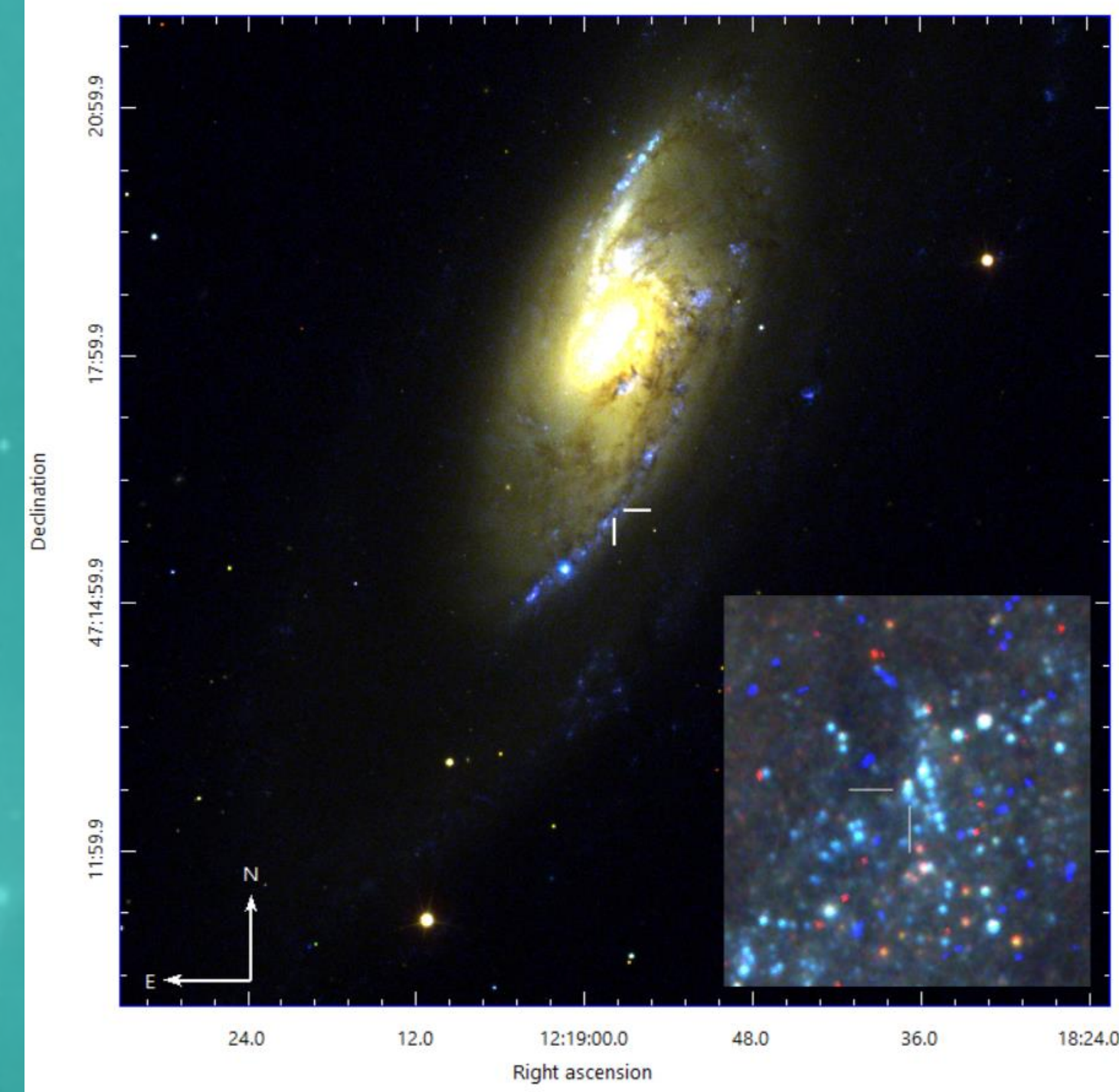

Fig 1: Three color SDSS image of NGC 4258. The position of X-3 is also shown on the image.

OBSERVATIONS AND DATA ANALYSIS

X-ray data

There are several XMM-Newton, Chandra, and Swift observations of NGC 4258 X-3 in the archives. The observations used in this study are summarized in Table 1. Standard analysis steps were done with Science Anaylsis Software (SAS, version 16.0.0) for XMM-Newton, Chandra Interactive Analysis of Observations (CIAO, version 4.9) for Chandra and XSELECT (version 2.4d) for Swift.

The count rate values of the ULX were calculated in the low (0.3 – 2.0 keV), high (2.0 – 8.0 keV) and total (0.3 – 10 keV) energy bands for all data in order to examine the long-term variability of the source. All XMM-Newton count rate values were taken from EPIC pn chip except XM2 data since X-3 was partially in the chip gap. The long-term light curves are given in Fig 2 and 3. Also long-term hardness ratio evolution is shown in Fig 4.

Spectral fittings were carried out with XSPEC package (version 12.9.1). Only Swift data were not used for spectral analyses due to low statistics. Flux values were calculated using CFLUX convolution model in XSPEC in the 0.3 – 10 keV energy band. The best fit parameters for PL and disk blackbody (DISKBB) models are given in Table 2. Energy spectra of X-3 in XM7 data are given in Fig 5. We also calculated bolometric luminosity values by integrating DISKBB model fluxes in the 0.01 – 100 keV energy range and estimate L_{bol} – T_{in} relation. The obtained figure is given in Fig 6. We found a best-fit relation of $L_{bol} \propto T_{in}^{4.4\pm0.9}$.

In XM1, XM2 data, PL model and in XM3, XM5, XM6, XM7 data, DISKBB model has given better fit by considering the reduced chi-square values. While in XM4 and C1 data the spectrum is well modeled with both models.

The mass of the compact object in the system might be estimated by considering that the source emits in the Eddington limit with highest luminosity . As seen in Table 2, X-3 has the highest luminosity in C1 data. Adopting this luminosity, the mass of the compact object in X-3 could be estimated as <40$M_\odot$. Also another mass value was calculated for the compact object by using DISKBB normalization parameter (5.5×10^{-3}). Assuming the spectral hardening κ = 1.7, inclination $i=60$ [11] the mass of the compact object was estimated as ~10 $M_\odot$.

Table 1: XMM-Newton, Chandra, and Swift obersvations

Label	ObsID	Date	Good Exp. (ks)
XMM-Newton			
XM1	0110920101	2000 Dec 8	16
XM2	0059140101	2001 May 6	9
XM3	0059140201	2001 Jun 17	10
XM4	0059140401	2001 Dec 17	12
XM5	0059140901	2002 May 22	14
XM6	0203270202	2004 Jun 1	47
XM7	0400560301	2006 Nov 17	59
Chandra			
C1	1618	2001.05.28	21
Swift XRT			
S1	00037259001	2008 Mar 1	10
S2	00037317001	2008 May 8	4
S3	00037317002	2009 Mar 9	4
S4	00037317003	2009 May 9	2
S5	00037259002	2014 May 21	2
S6	00037259005	2014 May 24	1
S7	00037259006	2014 May 25	2
S8	00060599001	2014 May 25	2
S9	00037259007	2014 May 30	2
S10	00037259009	2014 Jun 08	2
S11	00037259011	2014 Jun 18	0.03
S12	00037259012	2014 Jun 22	2
S13	00084408001	2015 Oct 18	2
S14	00084408002	2015 Oct 25	0.5
S15	00084408003	2015 Oct 28	0.6
S16	00081700001	2015 Nov 16	2
S17	00081700002	2016 Jan 10	2

Table 2: The best-fit spectral model parameters of NGC 4258 X-3.

| No.	N_H (10^{22} cm^{-2})	Γ	T_{in} (keV)	χ^2_ν (dof)	L_X (10^{39} erg s[-1])
		tbabs*powerlaw			
XM1	$0.39^{+0.04}_{-0.04}$	$2.15^{+0.14}_{-0.13}$	-	1.24 (35)	$1.83^{+0.17}_{-0.15}$
XM2	$0.55^{+0.06}_{-0.06}$	$2.27^{+0.15}_{-0.15}$	-	1.36 (24)	$4.19^{+0.47}_{-0.42}$
C1	$0.60^{+0.05}_{-0.05}$	$2.00^{+0.12}_{-0.12}$	-	0.72 (34)	$5.38^{+0.32}_{-0.32}$
XM3	$0.40^{+0.06}_{-0.05}$	$2.20^{+0.15}_{-0.15}$	-	0.79 (27)	$2.38^{+0.26}_{-0.25}$
XM4	$0.65^{+0.09}_{-0.09}$	$2.29^{+0.16}_{-0.15}$	-	0.92 (73)	$5.32^{+0.49}_{-0.47}$
XM5	$0.61^{+0.06}_{-0.06}$	$2.04^{+0.11}_{-0.11}$	-	1.62 (47)	$3.53^{+0.30}_{-0.29}$
XM6	$0.36^{+0.02}_{-0.02}$	$2.22^{+0.05}_{-0.05}$	-	0.71 (57)	$1.83^{+0.06}_{-0.06}$
XM7	$0.53^{+0.02}_{-0.02}$	$2.15^{+0.05}_{-0.05}$	-	1.27 (229)	$3.92^{+0.14}_{-0.14}$
		tbabs*diskbb			
XM1	$0.16^{+0.04}_{-0.04}$	-	$1.12^{+0.12}_{-0.10}$	1.81 (35)	$0.97^{+0.09}_{-0.08}$
XM2	$0.22^{+0.05}_{-0.05}$	-	$1.16^{+0.14}_{-0.12}$	1.52 (24)	$2.02^{+0.23}_{-0.23}$
C1	$0.32^{+0.05}_{-0.05}$	-	$1.34^{+0.13}_{-0.10}$	0.70 (34)	$3.14^{+0.18}_{-0.18}$
XM3	$0.10^{+0.06}_{-0.05}$	-	$1.18^{+0.13}_{-0.11}$	0.94 (27)	$1.22^{+0.13}_{-0.13}$
XM4	$0.33^{+0.08}_{-0.07}$	-	$1.16^{+0.10}_{-0.09}$	0.91 (73)	$2.64^{+0.24}_{-0.23}$
XM5	$0.29^{+0.06}_{-0.06}$	-	$1.33^{+0.12}_{-0.11}$	1.26 (47)	$2.04^{+0.17}_{-0.17}$
XM6	$0.13^{+0.04}_{-0.03}$	-	$1.09^{+0.12}_{-0.10}$	0.78 (57)	$0.98^{+0.10}_{-0.09}$
XM7	$0.25^{+0.02}_{-0.02}$	-	$1.29^{+0.04}_{-0.04}$	1.02 (229)	$2.24^{+0.08}_{-0.08}$
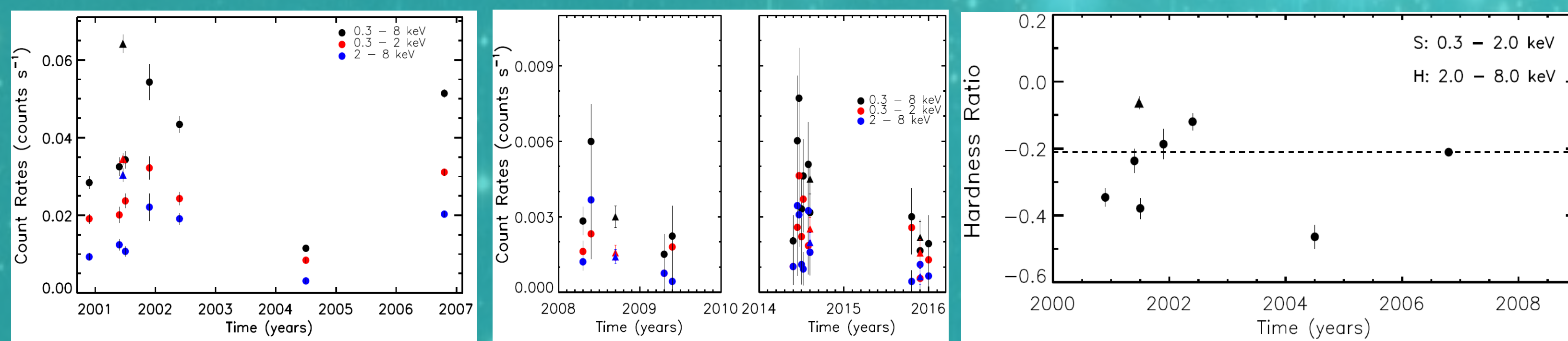
Fig 2: Long-term light curve of X-3 obtained with XMM-Newton and Chandra data. Filled circles and triangles represent XMM-Newton and Chandra data, respectively.
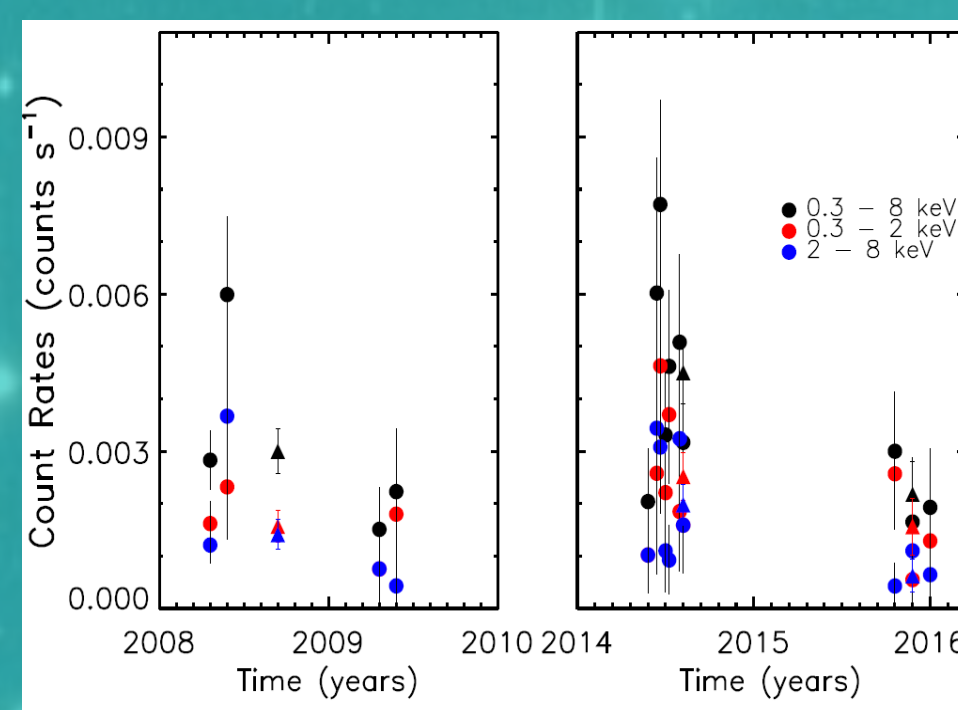

Fig 3: Long-term light curve of X-3 obtained using Swift data. Triangles represent combined Swift data.
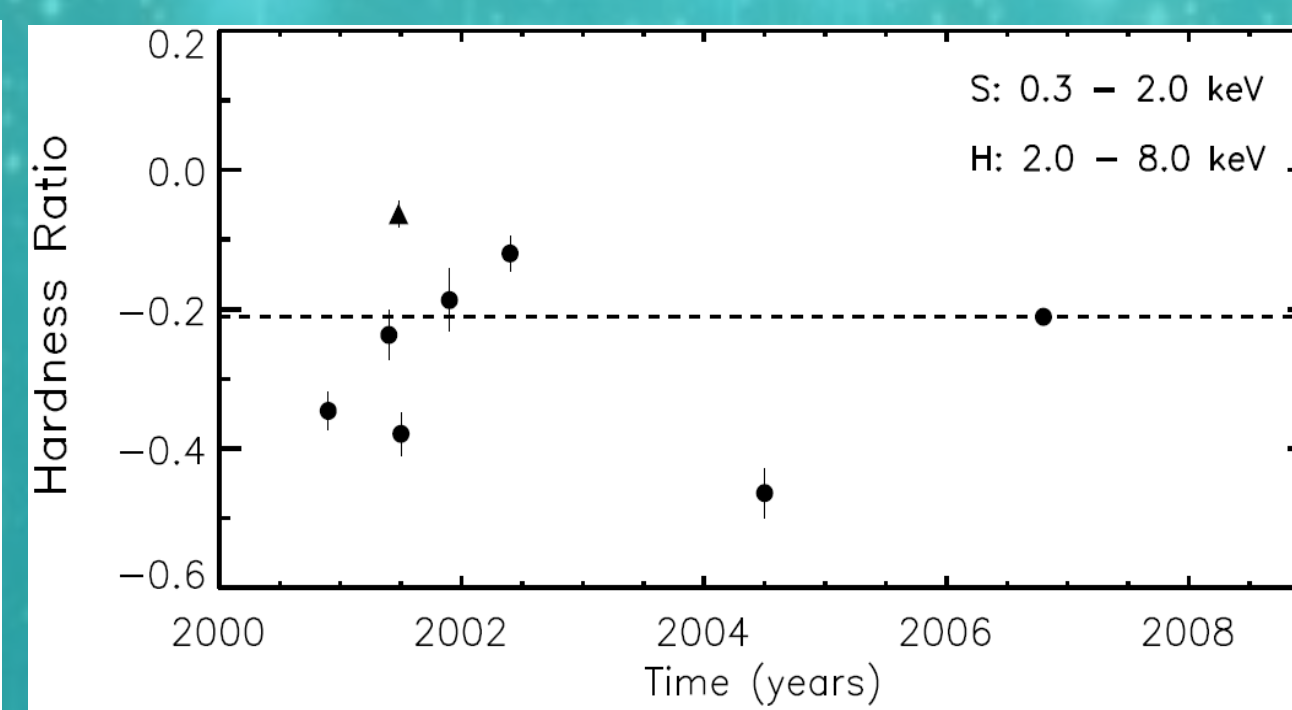

Fig 4: Long-term hardness ratio of X-3 obtained with XMM-Newton (circles) and Chandra (triangle) data.

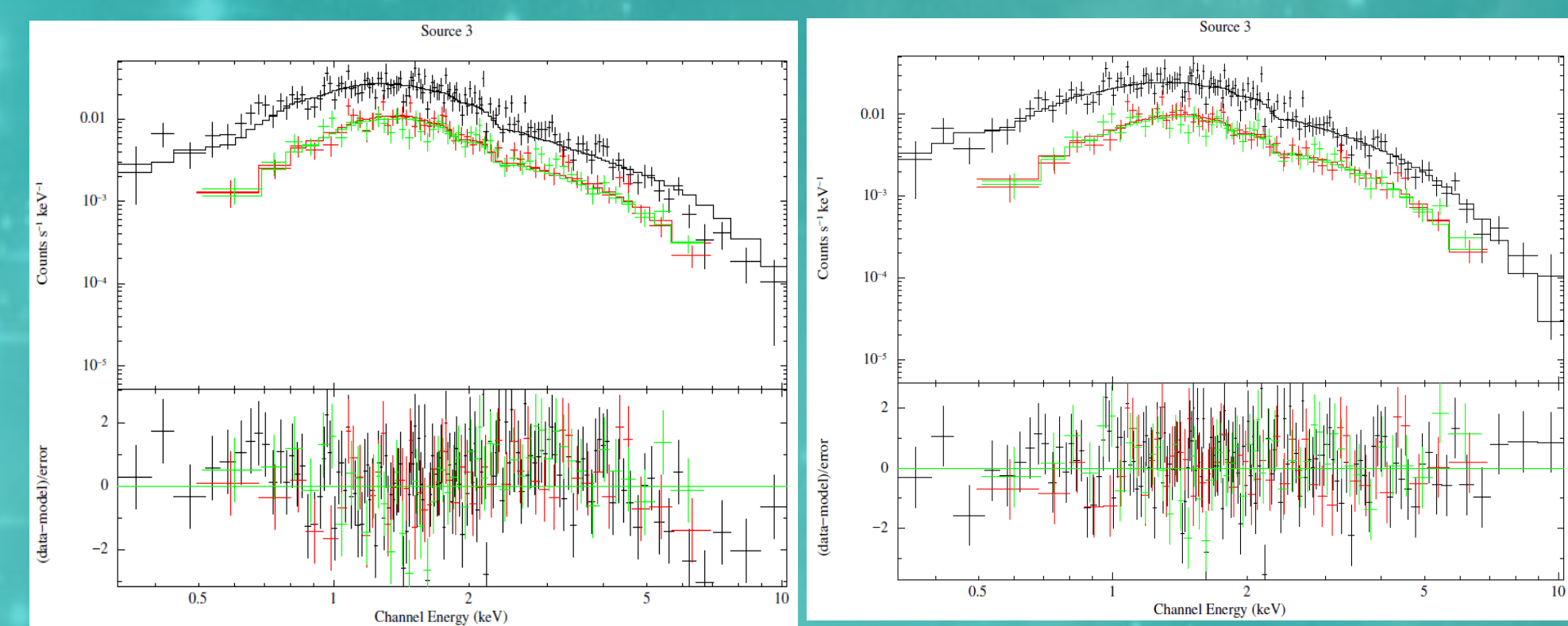
Fig 5: Energy spectra of X-3 in XM7 data (a) fitted with PL (left) DISKBB (right) models. The black, green and red data points represent EPIC pn, MOS1 and MOS2, respectively.
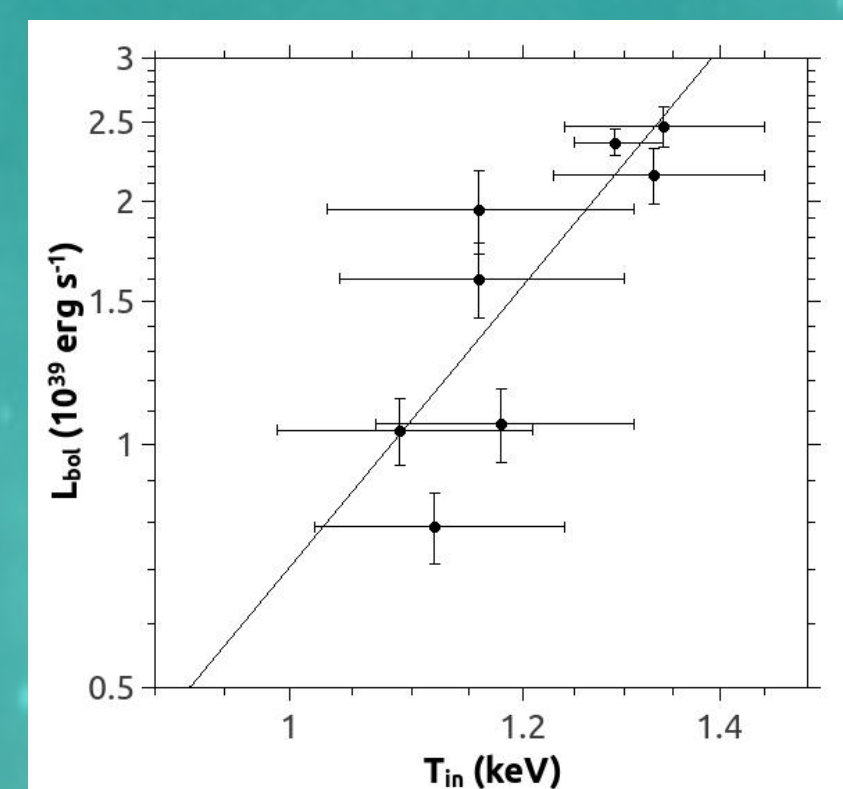

Fig 6: Bolometric luminosity versus innter temperatures. The solid line shows the best-fit relation of T α $L^{4.4\pm0.9}$

HST analysis

The HST/ACS F555W image were used to search optical counterpart of X-3. Astrometric matches between Chandra and HST were improved using one bright reference source and the position of the optical counterpart was derived as R.A. = 12 18 57.895, decl. = +47 16 07.530 with a 2σ positional error of 0.2 arcsec. The observation log of X-3 is given in Table 3.

In the error radius, three possible sources (Fig 7) were detected as counterpart candidates for X-3. PSF photometry were carried out to calculate magnitude values of the candidates with DOLPHOT software (version 2.0) [12]. Photometric results are given in Table 4.

To estimate the age of the counterpart candidates the color-magnitude diagrams (CMDs) were obtained and PARSEC isochrones were overplotted [13]. The obtained CMDs are given in Fig 8 and according to these diagrams, the age of the possible counterparts of X-3 are estimated as ~20-25 Myr for src1, ~20 Myr for src2 and ~40 Myr for src3. Assuming the optical emission is dominated by donor star, the spectral type of src1, src2 and src3 could be estimated as F2-F8 supergiant, A0-A7 supergiant and A3-A5 supergiant, respectively. Also the masses of candidates can be assessed from isochrones for src1, src2 and src3 are 11$M_\odot$, 10$M_\odot$ and 7$M_\odot$, respectively.

Table 3: Log of HST observations of NGC4258-X-3

Filter	ObsID	Date	Exp.
ACS/F435W	J9H807010	2009-12-03	360
ACS/F555W	J9H807020	2009-12-03	975
ACS/F814W	JC9V64020	2009-12-03	375
ACS/F435W	J9H807010	2009-12-14	360
ACS/F555W	J9H807020	2009-12-14	975
ACS/F814W	JC9V64020	2009-12-14	375

Table 4: Photometric results of X-3

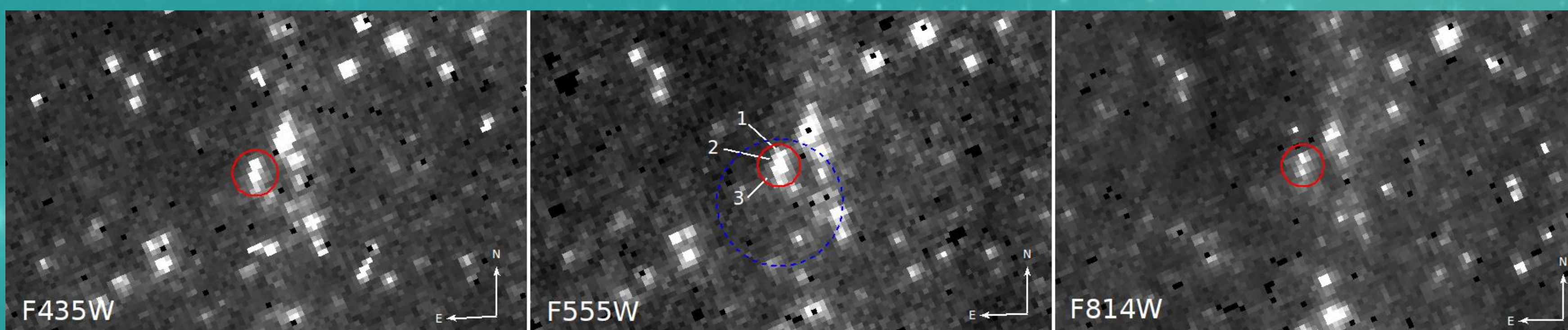| Source No.	Filter	VEGAmag	STmag	M_V	F ($\times 10^{-18}$) erg cm^{-2} s^{-1}
1	F435W	23.888 ± 0.039	23.906 ± 0.039	-5.75	1.01
	F555W	23.677 ± 0.035	23.617 ± 0.035		1.22
	F814W	22.902 ± 0.026	22.886 ± 0.026		2.50
2	F435W	23.634 ± 0.034	23.678 ± 0.034	-5.83	1.27
	F555W	23.603 ± 0.033	23.568 ± 0.033		1.31
	F814W	23.514 ± 0.041	23.499 ± 0.041		1.42
3	F435W	24.577 ± 0.061	24.620 ± 0.061	-4.84	0.53
	F555W	24.592 ± 0.064	24.553 ± 0.064		0.52
	F814W	24.306 ± 0.071	24.291 ± 0.071		0.68

Fig 7: The HST/ACS images of X-3. The blue –dashed circle represents 0.6 arcsec Chandra position error and red circles represent the corrected position of the source.
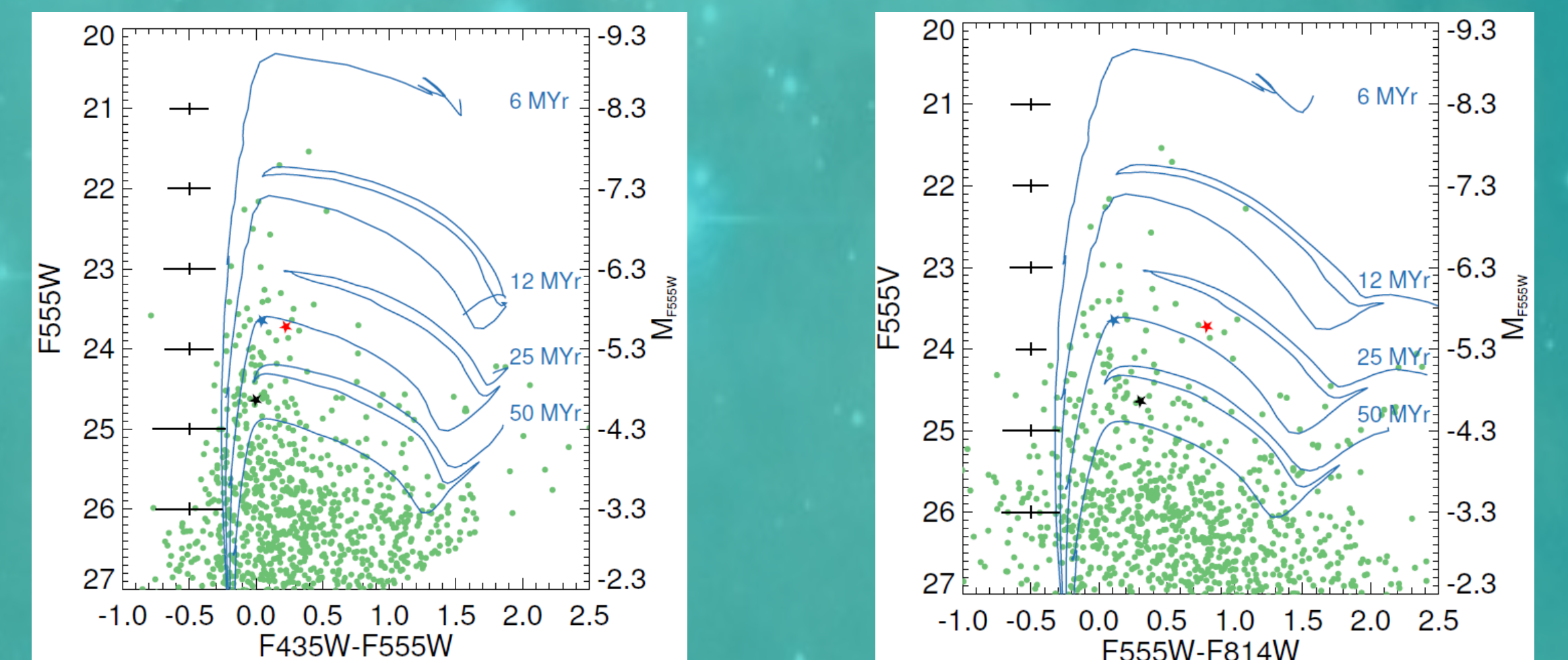

Fig 8: The CMDs for src1, src2 and src3 and for the field stars. Red, blue and black stars represent src1, src2 and src3, respectively. The magnitutes were corrected for extinction by E(B-V) = 0.016 [14].

DISCUSSION

ULX X-3 does not exhibit possible spectral variations. There are not distinct differences between the power-law model and the standard model to determine the spectral characteristic of ULX X-3 . However, the relation is expected optically thick standard accretion disk $L_{bol} \propto L^{4.4\pm0.9}$ was found with a correlation coefficient of ~0.8. Therefore it seems not very difficult to interpret the emission of ULX X-3 as being the result of a standard disk.

The best-fitting parameters to the models are in the range Γ ~ 2.0-2.3 for the PL model , and T_{in} ~1.1- 1.3 for the DISKBB model. This range of PL photon index is seen in the hard state and its very typical for ULXs which are detected by Chandra [15]. On the other hand, inner disk temperatures are a little high compared to Galactic BHBs in thermal dominated state which has disk temperatures between 0.7 and 1.1 keV [7]. Using the relation between inner disk radius and mass, we calculated a BH mass of M~10M☉ for a non-spinning BH. This indicates the possible stellar mass black hole in the ULX binary.

If we assume that the optical emission of X-3 is dominated by the companion star and we use the Schmidt–Kaler table [17] of intrinsic colors, then the probable spectral types of src 1, 2, and 3 can be estimated to be F2–F8, A0–A7, and A3–A5 supergiants, and the ages determined to be in the ranges 20-25Myr, 25Myr, and ~40 Myr, respectively.

The masses of the counterpart candidates are estimated from the PARSEC isochrones by taking into account their ages and absolute magnitudes as 11M☉ for src 1, 10 M☉ for src 2, and 7 M☉ for src 3. The mass ranges of the candidates are compatible with the donor stars of other ULXs [18].

References

[1] Poutanen et al. 2007 . MNRAS, 377, 1187
[2] Colbert & Mushotzky 1999. ApJ, 519, 89
[3] Feng & Soria 2011. NewAR, 55, 166
[4] Bachetti et al. 2014. Natur, 514, 202
[5] Israel et al. 2016. MNRAS, 462, 4371
[6] Fürst et al. 2016. ApJ, 831, L14
[7] Remillard & McClintock 2006. ARA&A, 44, 49
[8] Swartz et al. 2011. ApJ, 741, 49
[9] Wilson et al. 2001. ApJ, 560, 689
[10] Akyuz et al. 2013. AJ, 145, 67
[11] Maksimha et al. 2000. ApJ, 535, 632
[12] Dolphin 2000. PASP, 112, 1383
[13] Bressan et al. 2012. MNRAS, 427, 127
[14] Schelegel et al. 1998. ApJ, 500, 525
[15] Swartz et al. 2004. ApJS, 154, 519
[16] Tao et al. 2011. ApJ, 737, 81
[17] Aller et al. 1982. Landolt-Bornstein: Numerical data and Functional relationstip in Science and Technology vol2. New York, Springer.
[18] Patruno & Zampieri 2008. MNRAS, 386, 543